Atomic Parity Non-Conservation in Francium: The FrPNC Experiment at TRIUMF

S. Aubin([1]), E. Gomez([2]), J. A. Behr([3]), M. R. Pearson([3]), D. Sheng([4]), J. Zhang([4]), R. Collister([5]), D. Melconian([6]), Y. Zhao([7]), V. V. Flambaum([8]), G. D. Sprouse([9]), L. A. Orozco([4]), and G. Gwinner([5])

([1]) *Department of Physics, College of William and Mary, Williamsburg, VA 23187, USA*
([2]) *Institute of Physics, Universidad Autonoma de San Luis Potosi, San Luis Potosi, Mexico*
([3]) *TRIUMF, Vancouver, British Columbia V6T 2A3, Canada*
([4]) *Joint Quantum Institute, Department of Physics, and National Institute of Standards and Technology, College Park, Maryland 20742, USA*
([5]) *Department of Physics and Astronomy, University of Manitoba, Winnipeg, Manitoba R3T 2N2, Canada*
([6]) *Cyclotron Institute, Texas AM University, College Station, Texas 77843, USA*
([7]) *Laser Spectroscopy Laboratory of Shanxi University, State Key Laboratory of Quantum Optics and Quantum Optics Devices, Shanxi University, Taijuan, 030006, China*
([8]) *School of Physics, University of New South Wales, Sydney 2052, Australia*
([9]) *Department of Physics and Astronomy, SUNY Stony Brook, Stony Brook, New York 11794-3800, USA*

Summary. — The FrPNC collaboration is constructing an on-line laser cooling and trapping apparatus at TRIUMF to measure atomic parity non-conservation (PNC) and nuclear anapole moments in a series of artificially produced francium isotopes. Francium's simple electronic structure and enhanced parity violation make it a strong candidate for precision measurements of atomic PNC: the optical PNC and anapole-induced PNC effects are expected to be an order of magnitude larger in francium than in cesium. Atomic PNC experiments provide unique high precision tests of the Standard Model's predictions for neutral current weak interactions at very low energies. Furthermore, precision measurements of nuclear anapole moments probe inter-nucleon weak interactions within the nucleus.

PACS: 31.30.jg, 31.30.Gs, 32.70.Cs, 12.15.Ji, 21.10.Ky

1. – Introduction

Parity non-conservation (PNC) effects in atomic systems are unique low-energy probes of the electroweak sector of the Standard Model and of inter-nucleon weak interactions. While these atomic PNC effects are generally extremely small, they are enhanced sufficiently in heavy atoms for high precision spectroscopy to detect reliable PNC signals.

The FrPNC collaboration is constructing a dedicated laser cooling and trapping facility at the TRIUMF nuclear physics accelerator in Vancouver, Canada, for precision atomic PNC measurements in a string of francium isotopes.

The large enhancement of atomic PNC in francium makes these measurements sensitive to electroweak extensions of the Standard Model and can also provide strong constraints on PNC electron-quark couplings complementary to those obtained from electron scattering. More specifically, francium anapole moment measurements in a string of isotopes will assist in separating the isovector and isoscalar parts of the weak nucleon-nucleon interaction. Nuclear anapole moment measurements in cesium and thallium and low-energy nuclear parity violation experiments do not agree on a consistent set of weak nucleon-nucleon couplings [1, 2]. Anapole moment measurements in different francium isotopes will provide strong constraints on these weak couplings and an additional nuclear system with which to improve the existing theoretical frameworks [3, 4].

2. – Atomic PNC

Atomic PNC effects can be caused by either nuclear spin-independent (NSI) or nuclear spin-dependent (NSD) interactions between orbiting electrons and the nucleus. The largest PNC effect in heavy atoms is the NSI exchange of a Z^0 boson between an axial electron and a vector nucleon, as shown in Figure 1(a). In this process the PNC effect adds coherently for all nucleons: In the limit of an infinitely heavy nucleus, the PNC Hamiltonian for a single valence electron without radiative corrections is [5]

$$H_{PNC,NSI} \simeq \frac{G_F}{\sqrt{2}} \frac{Q_W}{2} \gamma_5 \rho(\vec{r}), \tag{1}$$

where $G_F = 10^{-5} m_p^{-2}$ is the Fermi constant, m_p is the proton mass, γ_5 refers to the Dirac matrix, $\rho(\vec{r})$ is the neutron distribution, and $Q_W = 2(\kappa_{1p} Z + \kappa_{1n} N)) \approx -N$ is the weak charge of the nucleus (Z and N are the number of protons and neutrons, respectively). The Standard Model gives the tree level values $\kappa_{1p} = \frac{1}{2}(1 - 4sin^2\theta_W)$ and $\kappa_{1n} = -\frac{1}{2}$ with the Weinberg angle $\sin^2\theta_W \sim 0.23$. NSI parity violation increases in heavy atoms as $Z^3 R$ with a relativistic enhancement factor R. The PNC effect in francium is expected to be 18 times larger than in cesium [6, 7].

In heavy atoms, the dominant contribution to NSD parity violation is the electromagnetic interaction of an electron with the nuclear anapole moment of the valence nucleon [Figure 1(b)]. The anapole moment is a parity violating nuclear electromagnetic moment due to inter-nucleon weak interactions. An electron interacting with a nuclear anapole moment has the following Hamiltonian

$$H_{PNC,\ NSD} = \frac{G_F}{\sqrt{2}} \frac{K \vec{I} \cdot \vec{\alpha}}{I(I+1)} \kappa_{a,i} \delta(\vec{r}) \text{ , with } \kappa_{a,i=n,p} = \frac{9}{10} g_i \frac{\alpha \mu_i}{m_p \widetilde{r}_0} A^{2/3}, \tag{2}$$

where $K = (I + 1/2)(-1)^{I-l+1/2}$, l is the orbital angular momentum of the valence nucleon, I is the nuclear spin, $\overrightarrow{\alpha}$ are Dirac matrices, and $\delta(\vec{r})$ indicates that the anapole moment produces a contact interaction for the electron dictated by the valence nucleon distribution. $\kappa_{a,i=n,p}$ is the effective interaction constant for the anapole moment produced by a valence neutron or proton, respectively. α is the fine structure constant, μ_i is the magnetic moment of the valence nucleon in nuclear magnetons, $\widetilde{r}_0$=1.2 fm is

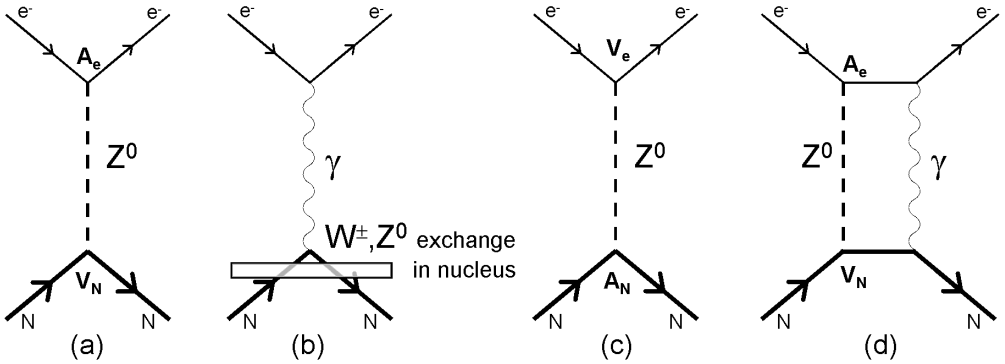

Fig. 1. – Atomic PNC processes. (a) The strongest PNC interaction in NSI optical PNC is the exchange of a Z^0 boson between an axial vector electron current and a vector nucleon current. (b) The largest NSD PNC effect in heavy atoms is produced by the anapole moment of the nucleus. The remaining two diagrams provide much smaller contributions to NSD PNC: (c) NSD Z^0 exchange between an axial vector nucleon current and a vector electron current, and (d) NSI Z^0 exchange in combination with the hyperfine interaction.

the nucleon radius, and $A = Z + N$ is the atomic mass. While NSD Z^0 exchange and NSI Z^0 exchange in combination with the hyperfine interactions, shown respectively in Figures 1 (c) and (d), produce NSD parity violation, their contribution is calculated to be more than an order of magnitude smaller than that due to the anapole moment. The anapole-induced PNC effect increases in heavy atoms as $Z^{8/3}R$ [5, 8]. The NSD parity violation in francium is expected to be 11 times larger than in cesium [9].

3. – Experimental Implementation

The FrPNC collaboration is preparing experiments to measure both optical PNC and nuclear anapole moments in a series of francium isotopes. TRIUMF produces the isotopes by spallation of a uranium carbide target with 500 MeV protons at the ISAC facility. A beamline will transport the francium to the laser laboratory, where it will be laser cooled and trapped in preparation for experiments. The proposed PNC experiments in Fr measure the degree of PNC-induced mixing of the $|s\rangle$ and $|p\rangle$ opposite parity wavefunctions with parity-forbidden transitions. The weak mixing angle can be extracted from an optical PNC measurement of the parity forbidden E1 transition between the $7s$ and $8s$ levels [Figure 2(a)], originally developed by Wieman and co-workers for cesium [10]. Nuclear anapole moments are measured with parity-forbidden microwave E1 transitions between the hyperfine manifolds of the $7s$ level [Figure 2(a)] [11] or through the dependence of optical PNC on the initial and final hyperfine states [10].

The PNC signal is the change in the "forbidden" transition rate upon the reversal of the handedness of the experiment, defined by three orthogonal external fields. In the optical PNC experiment, the momentum $\vec{k}$ of the excitation photon, an external Stark shift electric field $\vec{E}_{Stark}$, and a magnetic field $\vec{B}_{DC}$ determine the sign of the transition rate change, which is proportional to $\vec{B}_{DC} \cdot (\vec{k} \times \vec{E}_{Stark})$ [Figure 2(b)]. Similarly, in the anapole moment measurement, the population transfer between the hyperfine levels upon application of an electric microwave field $\vec{E}_{RF}$ is proportional to $\vec{B}_{DC} \cdot (\vec{B}_{\pi/2} \times \vec{E}_{RF})$. A microwave magnetic field $\vec{B}_{\pi/2}$ targeting an M1 transition is used to put the atoms in

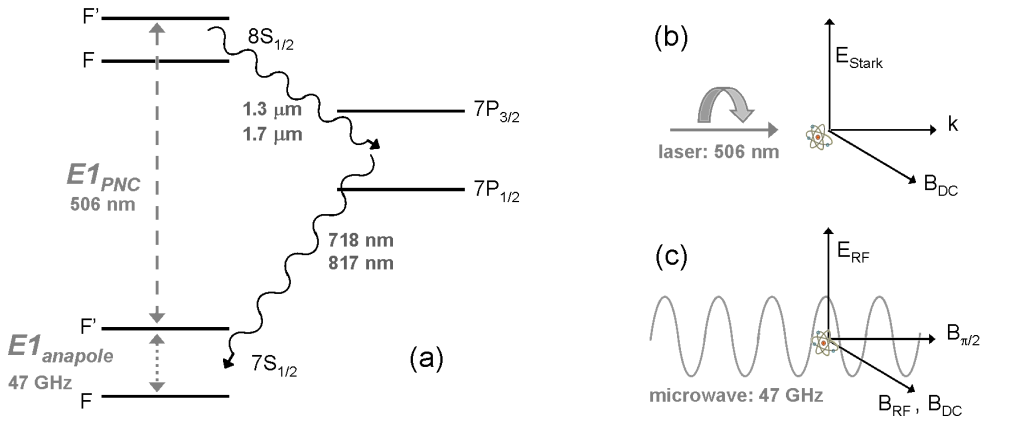

Fig. 2. – Francium energy levels and coordinate-system-defining vectors. (a) The $7s$, $8s$, and $7p$ energy levels francium relevant for the PNC measurements: the optical PNC method measures the parity forbidden transition between the $7s$ and $8s$ levels, while the anapole moment experiment measures the NSD parity forbidden transition between the hyperfine manifolds of the 7s level. External electromagnetic field vectors are used to define a coordinate system for the apparatus: The handedness of the coordinate system can be changed by flipping any one of the defining fields in (b) the optical PNC and (c) anapole moment experiments.

an initial equal superposition of two upper and lower hyperfine states (see Figure 2(c)).

The PNC-induced E1 transitions (parity-forbidden) used to measure NSI and NSD parity violation are generally accompanied by parity-allowed M1 transitions that mimic these E1 transitions. In the case of the optical PNC measurement on the $7s$ to $8s$ transition, the accompanying M1 transition is strongly suppressed, and is not expected to be an important source of systematic uncertainty. In the anapole moment measurement, the accompanying microwave M1 transition is nine orders of magnitude larger than the PNC-induced E1 transition, and so must be strongly suppressed. We plan to employ three methods to sufficiently suppress this unwanted M1 transition to an acceptable level [11]: a) We place the atoms at an electric field anti-node of the standing wave microwave driving field, which is a magnetic field node (the driving magnetic field is zero); b) the orientation of the microwave field polarization is chosen so that the magnetic component can only drive an off-resonance $\Delta m_F = 0$ transition, whereas the PNC-induced E1 transitions require $\Delta m_F = \pm 1$; finally, because of the spatial extent of the cold atomic cloud placed at the microwave magnetic field node, the atoms will experience some unwanted M1 transitions, but the motion of the atoms will tend to average out this effect, due to the π phase flip of M1 field at the node.

4. – PNC measurements with multiple isotopes

The availability of a range of francium isotopes is crucial for reducing nuclear physics uncertainties. Accurate extraction of the weak-mixing angle from an optical PNC measurement and of isoscalar and isovector weak nucleon-nucleon interaction parameters from an anapole measurement will benefit significantly from conducting a series of measurements in a string of isotopes in order to account for uncertainty in nuclear structure and the neutron skin thickness [12]. Existing efforts to directly measure the neutron

skin thickness in ^{208}Pb are important for reducing this source of systematic uncertainty [13, 14] in the extraction of the weak mixing angle. Furthermore, the collaboration is continuing laser spectroscopy measurements of hyperfine anomalies in a number of francium isotopes in order to constrain the change in neutron skin radius over the range of isotopes [15]: Variations in the ratio of the hyperfine A coefficients for the $7S_{1/2}$ and $7P_{1/2}$ levels for different francium isotopes are primarily due to variations in the magnetization radius of the nucleus. These hyperfine anomaly measurements provide a means of probing the magnetization distribution due to the different overlap of the $S_{1/2}$ and $P_{1/2}$ electronic wavefunctions with an extended nucleus. The combination of hyperfine anomaly measurements in francium isotopes with the accelerator-based neutron radius measurements in lead will strongly constrain the neutron skin in francium.

5. – Outlook

The FrPNC collaboration has completed construction of a radio-frequency shielded laser laboratory room in the ISAC hall of TRIUMF and is installing an on-line laser cooling and trapping apparatus for francium. The ISAC facility has successfully generated francium isotopes at rates in the range of $10^7 - 10^8$ Fr/s for $^{206-213}$Fr and $^{220-222}$Fr: these rates should permit the accumulation of laser-cooled samples of more than 10^6 Fr atoms [16], which are necessary for achieving large anapole PNC signals with projected fundamental signal-to-noise ratios in the range of 20 for 1 s of integration [11].

* * *

The authors thank the TRIUMF/ISAC francium production team. The collaboration gratefully acknowledges support by DOE, NSF, NSERC, and TRIUMF.

REFERENCES

[1] W. C. Haxton and C. E. Wieman, *Annu. Rev. Nucl. Part. Sci.*, **51** (2001) 261.
[2] J. A. Behr and G. Gwinner, *J. Phys G: Nucl. Part. Phys.*, **36** (2009) 033101.
[3] B. Desplanques, J. F. Donoghue, and B. R. Holstein, *Ann. Phys. (N.Y.)*, **124** (1980) 449.
[4] M. J. Ramsey-Musolf and S. A. Page, *Ann. Rev. Nucl. Par. Sci*, **56** (2006) 1.
[5] I. B. Khriplovich,, *Parity Nonconservation in Atomic Phenomena*, Gordon and Breach, New York, 1991.
[6] V. A. Dzuba, V. V. Flambaum, and O. P. Sushkov, *Phys. Rev. A*, **51** (1995) 3454.
[7] M. S. Safronova and W. R. Johnson, *Phys. Rev. A*, **62** (2000) 022112.
[8] V. V. Flambaum, I. B. Khriplovich, and O. P. Sushkov, *Phys. Lett. B*, **146** (1984) 367.
[9] E. Gomez, L. A. Orozco, and G. D. Sprouse, *Rep. Prog. Phys.*, **69** (2006) 79.
[10] C. S. Wood, S. C. Bennett, D. Cho, B. P. Masterson, J. L. Roberts, C. E. Tanner, and C. E. Wieman, *Science*, **275** (1997) 1759.
[11] E. Gomez, S. Aubin, G. D. Sprouse, L. A. Orozco, and D. P. DeMille, *Phys. Rev. A*, **75** (2007) 033418.
[12] B. A. Brown, A. Derevianko, and V. V. Flambaum, *Phys. Rev. C*, **79** (2009) 035501.
[13] PREX experiment: http://hallaweb.jlab.org/parity/prex; R. Michaels, talk, PAVI 2011 conference, Rome, Italy (2011).
[14] A. Tamii *et al.*, *Phys. Rev. Lett.*, **107** (2011) 062502.
[15] J. S. Grossman, L. A. Orozco, M. R. Pearson, J. E. Simsarian, G. D. Sprouse, and W. Z. Zhao, *Phys. Rev. Lett.*, **83** (1999) 935.
[16] S. Aubin, E. Gomez, L. A. Orozco, and G. D. Sprouse, *Rev. Sci. Instrum.*, **2003** (4352) .